Chemosphere 299 (2022) 134424

Contents lists available at ScienceDirect

Chemosphere

journal homepage: www.elsevier.com/locate/chemosphere

Terrestrial mercury and methylmercury bioaccumulation and trophic transfer in subtropical urban forest food webs

Fudong Zhang [a,b], Zhidong Xu [b], Xiaohang Xu [b,c], Longchao Liang [a], Zhuo Chen [a,**], Xian Dong [a], Kang Luo [b,d], Faustino Dinis [e], Guangle Qiu [b,*]

[a] School of Chemistry and Materials Science, Guizhou Normal University, Guiyang, 550001, China
[b] State Key Laboratory of Environmental Geochemistry, Institute of Geochemistry, Chinese Academy of Sciences, Guiyang, 550081, China
[c] Key Laboratory of Karst Georesources and Environment, Ministry of Education, College of Resources and Environmental Engineering, Guizhou University, Guiyang, 550025, China
[d] Ailaoshan Station for Subtropical Forest Ecosystem Studies, Chinese Academy of Sciences, Jingdong, 676200, China
[e] College of Agriculture, Guizhou University, Guiyang, 550025, China

HIGHLIGHTS

- Urban forest food web of plants-insects-spiders/nestlings was determined.
- Songbird nestlings exhibited elevated total mercury and methylmercury concentrations.
- Trophic magnification slope suggested a distinct transfer of methylmercury along determined food chain.

GRAPHICAL ABSTRACT

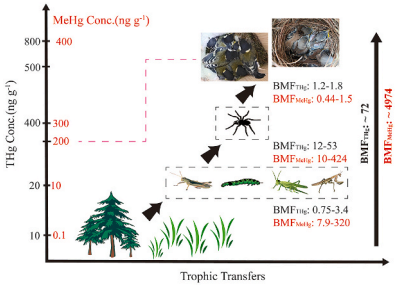

ARTICLE INFO

Handling Editor: Milena Horvat

Keywords:
Terrestrial mercury and methylmercury
Biomagnification
Stable isotopes
Urban forest's food webs

ABSTRACT

As the "lungs of the city", urban forests can improve air quality by absorbing air pollutants, becoming hotspots for mercury (Hg) pollution from anthropogenic activities. However, the bioaccumulation and transfer of Hg in the urban forest food web are unclear. In this study, total mercury (THg) and methylmercury (MeHg) concentrations, as well as the stable isotopes of carbon ($\delta^{13}C$) and nitrogen ($\delta^{15}N$) in organisms with different trophic levels (TLs) were investigated in a mid-subtropical urban forest of the Changpoling Forest Park (CFP) in Guiyang City, Guizhou Province, southwestern China. The results showed that THg and MeHg among all taxa ranged from 5.6 to 1267 ng g^{-1} and 0.046–692 ng g^{-1}, respectively. MeHg% (% of Hg present as MeHg) at different TLs exhibited a wide range of 5.0–69% on average. Both THg and MeHg increased with the TLs from plants to nestling birds, indicating distinct biomagnification through the food web of grasses/pine needles - grasshoppers/caterpillars/katydids/mantis - spiders/songbird nestlings. The trophic magnification slope (TMS) of THg and MeHg were 0.18 ± 0.05 and 0.37 ± 0.08, respectively, suggesting both of them significantly increase along food webs. These findings improve the understanding of biogeochemical Hg cycles in terrestrial food webs and highlight the impacts of terrestrial MeHg on nestling birds.

* Corresponding author.
** Corresponding author.
E-mail addresses: chenzhuo19@163.com (Z. Chen), qiuguangle@vip.skleg.cn (G. Qiu).

https://doi.org/10.1016/j.chemosphere.2022.134424
Received 4 January 2022; Received in revised form 22 March 2022; Accepted 23 March 2022
Available online 26 March 2022

1. Introduction

Mercury (Hg) is a persistent, global pollutant that can be transported thousands of miles in the atmosphere before being deposited onto the ground and in water (Driscoll et al., 2013; Fitzgerald et al., 1998), where it transforms into the more toxic organic form, methylmercury (MeHg), and can cause extensive issues for ecosystems. MeHg is highly neurotoxic, bioavailable, and readily biomagnified in biota at high trophic levels via food chains, posing great public concern (Abeysinghe et al., 2017; Horvat et al., 2003; Hsu-Kim et al., 2018; Scheuhammer et al., 2007). The bioaccumulation and biomagnification of Hg along food webs in aquatic ecosystems have been well documented (Driscoll et al., 2007; Gentes et al., 2021; Horvat et al., 2014; Kidd et al., 2012; Lavoie et al., 2013; Watras et al., 1998). Since Cristol et al. (2008) first reported that terrestrial songbirds could accumulate aquatic Hg by preying on riparian spiders, the accumulation and transfer of Hg in terrestrial food webs have drawn considerable attention (Abeysinghe et al., 2017; Rimmer et al., 2010; Tsui et al., 2012, 2019; Yung et al., 2019; Zhang et al., 2010).

Generally, food web structures, trophic levels, and diets can affect the bioaccumulation of Hg in biota (Adams et al., 2020; Driscoll et al., 2007; Tsui et al., 2012). Moreover, basal resource is another important factor that plays a crucial role in driving Hg transfer and bioaccumulation among organisms (Eagles-Smith et al., 2018; Rodenhouse et al., 2019; Tsui et al., 2019; Willacker et al., 2019). Recent studies on Hg in food webs of forest ecosystems have shown that significant Hg bioaccumulation and biomagnification occurs in organisms at high trophic levels, even at low basal Hg loadings (Luo et al., 2020; Li et al., 2021; Tsui et al., 2019). However, the mechanism of underlying the bioaccumulation of Hg, especially MeHg, in organisms of terrestrial food webs remains unclear.

Stable isotopes of carbon ($\delta^{13}C$) and nitrogen ($\delta^{15}N$) are powerful tools to decipher dietary sources and trophic positions in food webs (Post, 2002; Fry, 2006). Values of $\delta^{13}C$ have been used to elucidate energy flows to consumers and typically differentiate between C3 and C4 plants. Isotope ratios of $\delta^{15}N$ tend to increase from food source to consumer, and thus, are most frequently used as trophic position indicators. As such, the investigation of $\delta^{13}C$ and $\delta^{15}N$ may greatly advance the understanding of food web structures and relationships between Hg and distinct trophic levels (Tsui et al., 2019; Luo et al., 2020; Gentes et al., 2021).

Urban forests are tree-dominated ecosystems located in urban and peri-urban areas, comprising of street trees, trees in parks and gardens, and trees in derelict corners (FAO, 2016). Urban forests are referred to as the "lungs of the city" due to their significant impact on urban water, heat, and pollutant cycles (Livesley et al., 2016). Since trees reduce gaseous and particulate pollutants, urban forests may exhibit greater concentrations of toxic metals and be hotspots for various air pollutants from anthropogenic activities (Niu et al., 2011; Richardson and Moore, 2020; Zhou et al., 2016). Many studies have revealed that forests are globally important sinks for Hg deposition from the atmosphere (Obrist et al., 2021; Wang et al., 2016, 2020). As such, further investigation of the distribution and bioaccumulation characteristics of THg and MeHg in the biota of these forests may be highly informative.

China is undergoing explosive growth in urban forests due to rapid urbanization and economic development. Significant quantities of urban forest can improve air quality by absorbing air pollutants. Simultaneously, those captured and sequestered toxins may, in turn, affect biota within the ecosystem, contributing to increased contamination. However, few studies have focused on the bioaccumulation and transfer of THg and MeHg in the food chains of urban forests.

Avian species at higher trophic levels are extremely sensitive to Hg exposure, even at very low concentrations (Jackson et al., 2015; Li et al., 2021). Songbird feathers have been widely used as efficient and effective indicators of Hg contamination, as sampling is non-destructive and non-invasive (Ma et al., 2021; Peterson et al., 2019). However, the variability in Hg among and within individual feathers is high (Low et al., 2020; Peterson et al., 2019). In contrast to adults, nestling feathers are a more suitable indicator of Hg accumulation (Zabala et al., 2019). They are easier to collect, and the simple transmission process in the food webs. Nestling feathers may better reflect the characteristics of food composition, and thus, may provide better quantification of Hg biomagnification in songbirds (Luo et al., 2020).

To understand the accumulation and transfer of Hg in urban forest food webs, this study selected a mid-subtropical urban forest in Changpoling Forest Park (CFP) in Guiyang City, the capital of Guizhou Province in southwestern China, as the study area. Measurements of THg and MeHg and the stable isotopes of carbon ($\delta^{13}C$) and nitrogen ($\delta^{15}N$) were conducted in a range of organisms. The objectives were to (1) reveal the distribution characteristics of THg and MeHg in soils, plants, invertebrates, and nestling birds across the urban forest food web, (2) identify the food web structure in urban forest via the stable isotopes of $\delta^{13}C$ and $\delta^{15}N$, and (3) elucidate the bioaccumulation and transfer of THg and MeHg in the urban forest food web.

2. Materials and methods

2.1. Study area

CFP (106°39′10″E−106°40′10″E, 26°38′45″N-26°40′00″N) is located in northwestern Guiyang, which is the capital city of Guizhou Province, in southwestern China. The CFP, covers an area of 1294.2 ha, with an altitude of 1203–1370 m. It is characterized by a mid-subtropical humid monsoon climate, and has abundant biological resources. It has an annual average air temperature of 13.6 °C and annual average precipitation of 1200 mm. The forest cover of the park is 82.96% and it is dominated by coniferous forest. The main tree species are *Pinus massoniana* and *Pinus armandii*.

Songbirds are top predators, and their nestling feathers were used in this study to reveal the biomagnification and transfer of Hg in the urban forest food web. Approximately 170 artificial nest boxes were set up on pine trees in CFP at the April 2020 to collect feathers from nestling birds. All nest boxes were set up about 2.5 m above ground level with a distance of more than 10 m between two boxes. The main species of songbird breeds in the artificial nest boxes were the Green-backed Tit (*Parus monticolus,* GbT) and the Russet Sparrow (*Passer rutilans,* RS). These songbirds feed their nestlings by preying on insects and other invertebrates dwelling within nearby pine trees. No obvious water sources, such as springs, ponds, creeks, or rivers were observed near the experimental nest box plots (Fig. 1).

2.2. Sampling and sample preparation

Samples of nestling feathers, invertebrates, plants, and surface soils were systematically collected during the songbird breeding season from mid-April to the end of July 2020.

A total of 91 feather samples from individual nestlings were collected from 23 broods (GbT: n = 16; RS: n = 7), 70 were from GbT and 21 were from RS. The secondary flight feathers on both sides were non-invasively sampled when the nestlings reached an age of 12–15 days. After collection, the nestlings were safely returned to their nest boxes. All sampled feathers were stored in clean polyvinyl chloride (PVC) bags and then transferred to the laboratory and stored in a refrigerator (−20 °C) until further processing.

For the non-avian biota samples, spiders (*Araneae*, n = 14), katydids (*Tettigoniidae*, n = 6), mantis (*Mantodea*, n = 4), grasshoppers (*Orthoptera*, n = 24), and caterpillars (*Lepidoptera*, n = 3) were collected using sweep nylon nets. These taxa represent the food sources of songbirds. All collected invertebrates were put into gauze-covered centrifuge tubes in coolers with ice bags and were then transferred to the laboratory and stored in a refrigerator (4 °C) until further processing. Simultaneously, surface forest soil (0–10 cm, n = 30), newly grown pine needles (*Pinus*

massoniana, n = 11), and dominant growing grasses (*Arthraxon prionodes*, n = 18) were also collected adjacent to the nest boxes.

Nestling feathers were ultrasonically washed with tap water, detergent, acetone, and deionized water in the laboratory. After thorough cleaning, all feathers were air-dried and cut into 1–2 mm lengths using ceramic scissors for analysis. The invertebrate samples were starved for 24 h and then their excrements and traces of food in the digestive system were removed as these may impact the chemical analyses. The samples were then gently washed with deionized water and freeze-dried (−80 °C, LGJ-10, China). Next, the were ground into a homogenized powder with an agate mortar and pestle before being stored in PVC bags for analysis. For individual invertebrates with a very low mass, composited samples were obtained by mixing the homogenized powders of at least 10 individuals.

Plant samples were thoroughly cleaned with tap and deionized water, then dried at 60 °C to a constant weight. They were then ground into a homogenized powder with a pulverizer (IKAA11, Germany), sieved through 40-mesh (0.420 mm), and stored in PVC bags for analysis. Soil samples were air-dried in a clean and ventilated environment, ground into a homogenized powder with a ceramic mortar and pestle, sieved through 200 mesh (0.075 mm), and stored in PVC bags for analysis.

2.3. Analytical methods

2.3.1. THg and MeHg analyses

Feathers

The concentrations of THg and MeHg in nestling feathers were determined following the methods recommended by Hammerschmidt and Fitzgerald (2005), Hintelmann and Nguyen (2005), Tsui et al. (2018, 2019), and USEPA Method 1631E and 1630, due to the low mass of the samples. In brief, approximately 0.005–0.01 g feathers were weighed into a 50 mL centrifuge tube and then digested with 5 mL 4 M HNO_3 at 60 °C for 12 h. For MeHg analysis, approximately 2 mL of digested solution was separated, followed by addition of acetate buffer (2 M, 0.2 mL) to adjust the pH to 4.9, then determined with the gas chromatography-cold vapor atomic fluorescence spectrometry (GC-CVAFS, Brooks Rand Model III, USA) following the USEPA Method 1630 (US EPA, 1998) and Liang et al. (1994). For THg analysis, the remaining 3 mL of digested solution was again added to 3 mL of concentrated HNO_3 at 95 °C for 3 h, followed by 0.5 mL BrCl oxidation, $NH_2OH{\cdot}HCl$ neutralization, and $SnCl_2$ reduction, then purge and flow into gold amalgam traps, thermal desorption, finally determined by using the cold vapor atomic fluorescence spectrometry (CVAFS, Brooks Rand Model III, USA) following the USEPA Method 1631E (US EPA, 2002). For THg, the limit of determination (LOD, mean value of blank plus 3SD) and limit of quantification (LOQ, mean value of blank plus 10SD) were 0.36 ng g^{-1} and 0.68 ng g^{-1} in nestling feathers.

Invertebrates, plants, and soil

The THg in invertebrates, plants, and soil was determined using the Direct Mercury Analyzer (DMA-80, Milestone, Italy) following the USEPA Method 7437 (US EPA, 2007). The instrument detection limit was 0.005 ng, and the method LOD was 0.20 ng g^{-1} and the LOQ was 0.46 ng g^{-1}.

The MeHg in invertebrates, plants, and soil was also determined using a GC-CVAFS (Brooks Rand Model III, USA) following the USEPA Method 1630 (US EPA, 1998). In brief, invertebrates and plants were digested with 5 mL 25% (m/v) KOH–MeOH solution at 75 °C for 3 h. Then 10 mL of CH_2Cl_2 was added, and the solution was shaken for 1 h, centrifuged for 25 min at 3000 rpm, and then back-extracted into water phase. After dilution, the MeHg was determined with GC-CVAFS. Soil samples were extracted with 2 mL of 1 M $CuSO_4$, 8 mL of 3 M HNO_3, and

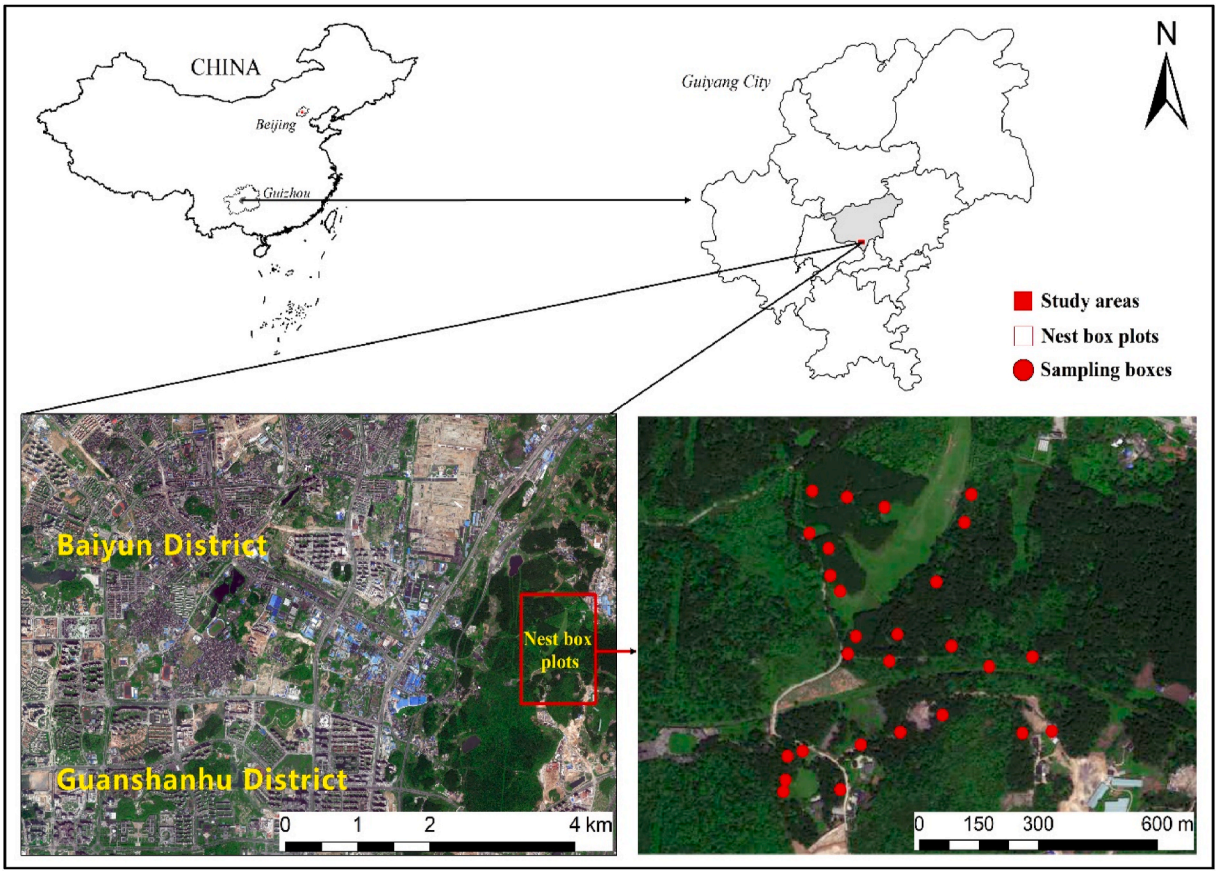

Fig. 1. Sampling sites in the Changpoling Forest Park (CFP), Guiyang, southwest China.

10 mL of CH_2Cl_2 following the method reported by Liang et al. (2004), and determined using a GC-CVAFS as for the invertebrate and plant samples. The LOD and LOQ were 0.0060 ng g^{-1} and 0.010 ng g^{-1}.

2.3.2. Stable isotopes analyses

Stable isotope compositions ($\delta^{13}C$ and $\delta^{15}N$) were determined using a homogenized powder sample that was combusted in tin cups under continuous flow with an EA2000 elemental analyzer (Thermo Scientific, Germany), linked with a MAT253 isotope ratio mass spectrometry (Thermo Scientific, Germany). Cellulose (IAEA-C_3, $\delta^{13}C = -24.7‰$) and KNO_3 (IAEA-NO_3, $\delta^{15}N = 4.7‰$) were used as the sample standards to calibrate $\delta^{13}C$ and $\delta^{15}N$, respectively. The analytical precision for $\delta^{13}C$ and $\delta^{15}N$ was smaller than 0.1‰, and the results were presented as ratios in standard δ notation (‰) according to the following equation:

$$\delta X = \left(R_{sample} / R_{standard} - 1\right) \times 1000‰ \quad (1)$$

where X is to $\delta^{13}C$ or $\delta^{15}N$ and R is the abundance ratios of $^{13}C/^{12}C$ or $^{15}N/^{14}N$. The standards were Vienna Pee Dee Belemnite (V-PDB) for carbon, and atmospheric nitrogen (N_2) for nitrogen.

2.3.3. QA/QC

Quality assurance and quality control (QA/QC) was accomplished with method blanks, duplicate samples (10%), and certificated reference materials (CRMs). The relative standard deviations (RSDs) in duplicate samples for THg and MeHg were 1.8–8.6% and 1.0–9.3%, respectively.

For THg, the CRMs of TORT-2 (lobster hepatopancreas, National Research Council Canada, Canada, Certified THg Value: 270 ± 30 ng g^{-1}), BCR 482 (epiphytic lichen, Certified THg Value: 480 ± 20 ng g^{-1}), and GSS-5 (red-yellow soils, Certified THg Value: 290 ± 30 ng g^{-1}) were employed, and the measured values were 272 ± 7.0 ng g^{-1} (n = 9), 484 ± 11 ng g^{-1} (n = 4), and 287 ± 5.1 ng g^{-1} (n = 14), with recoveries of 97.6–103%, 97.0–106%, and 96.4–102%, respectively.

For MeHg, the CRMs of ERM-CC580 (estuarine sediment, Certified MeHg Value: 75 ± 4.0 ng g^{-1}) and TORT-2 (Certified MeHg Value: 152 ± 13 ng g^{-1}) were employed, and the measured values were 78 ± 3.4 ng g^{-1} (n = 4) and 159 ± 4.0 ng g^{-1} (n = 5), with recoveries of 102–110% and 101–107%, respectively. Our measured CRM values were 101–110% times of the recommended values (no significant difference at the 95% confidence level), which were within the ranges observed in previous studies (95–110%) (Hintelmann and Nguyen, 2005; Tsui et al., 2012; Hammerschmidt and Fitzgerald, 2005; Horvat et al., 2014). Such small positive biases may be attributed to the slight variation of sensitivity (fluorescence signal) between each day (Azemard and Vassileva, 2021). We also evaluated the potential impact of the slightly positive bias on our key conclusions in the discussion section. In the present study, all data for THg and MeHg are reported in dry weights (d.w.).

2.4. Data analyses

2.4.1. Trophic level (TL)

The trophic level (TL) of each organism was calculated based on $\delta^{15}N$ and following the equation recommended by Post (2002):

$$TL = \left(\delta^{15}N_c - \delta^{15}N_{base}\right) / \Delta n + \lambda \quad (2)$$

where TL is the average TL of the species, $\delta^{15}N_c$ and $\delta^{15}N_{base}$ are the average $\delta^{15}N$ values of consumers and primary producers, respectively. Δn is the fractionation. A value of 3.4‰ is the average $\delta^{15}N$ trophic enrichment factor, which was widely used for food web analyses (Luo et al., 2020; Gentes et al., 2021). However, in the present study, a value of 3.7‰ was used as the fractionation between nestlings and diet (Becker et al., 2007). λ is the trophic position of the baseline organisms, which is considered as pine needle and grass in the present study. For the primary producers, λ was 1.

2.4.2. Biomagnification factor (BMF)

The values of biomagnification factor (BMF) values between predators and their prey were calculated on the basis of the following equations (Luo et al., 2020; Yung et al., 2019):

$$BMF_{(THg\ or\ MeHg)\ predator} = \frac{[THg\ or\ MeHg]_{predator}}{[THg\ or\ MeHg]_{prey}} \quad (3)$$

where $[THg\ or\ MeHg]_{predator}$ and $[THg\ or\ MeHg]_{prey}$ are the concentrations of THg or MeHg in the predator and prey, respectively.

2.4.3. Trophic magnification slope (TMS)

The trophic magnification slope (TMS) is the slope (b) of the regression between the $\log_{10}$ [THg] or $\log_{10}$ [MeHg] and $\delta^{15}N$ values of biota, which was calculated on the basis of the following equation (Lavoie et al., 2013):

$$\log_{10}[THg\ or\ MeHg] = b \times \delta^{15}N + a \quad (4)$$

The TMS is widely applied to quantify Hg biomagnification in food webs, and TMS>0 indicates significant biomagnification.

2.5. Statistical analyses

Statistical analyses were performed with Microsoft Excel 2019 (Microsoft Corporation, USA), RStudio version 4.1.2 (R Core Team 2021), and SPSS Statistics 25 (International Business Machines Corporation, USA). Figures were performed using Origin 2021 (Origin Lab Corporation, USA). Linear regression analysis was performed to produce estimates for the slope and intercept of the linear equation predicting the TMS results, as well as the strength and direction of the linear relationship between log [THg] and log [MeHg]. In each statistical test, $p < 0.05$ was considered statistically significant.

3. Results and discussion

3.1. THg and MeHg

The concentrations of THg and MeHg in the nestling feathers and invertebrates were all shown distinct variations, exhibiting wide ranges of 6.1–1267 ng g^{-1} and 0.28–692 ng g^{-1}, respectively (Table 1). For THg, the RS and GbT (the top predators) had the highest mean concentrations of 797 ± 221 ng g^{-1} and 521 ± 156 ng g^{-1}, respectively, followed by spiders (433 ± 45 ng g^{-1}). While katydids (37 ± 3.9 ng g^{-1}), caterpillars (32 ± 0.48 ng g^{-1}), and mantis (30 ± 5.6 ng g^{-1}) had the comparable low concentrations. Unexpectedly, mantis which are typically carnivorous insects, exhibited similar THg levels with herbivorous insects, which were distinctly different from other insectivores (Abeysinghe et al., 2017; Luo et al., 2020). Of all the taxa, the THg levels in grasshoppers were the lowest, with a mean of 8.2 ± 2.0 ng g^{-1} (Table 1, Fig. 2).

For MeHg, the RS showed the highest mean concentration (388 ± 156 ng g^{-1}) among all taxa, followed by spiders (263 ± 42 ng g^{-1}), GbT (115 ± 31 ng g^{-1}), katydids (25 ± 4.9 ng g^{-1}), mantis (17 ± 5.0 ng g^{-1}), caterpillars (1.6 ± 0.18 ng g^{-1}), and grasshoppers (0.62 ± 0.25 ng g^{-1}). The percentage of Hg present as MeHg (MeHg%) among taxa was distinct. Katydids, mantis, and spiders showed higher ratios (56–69%) than nestling feathers (24–49%), while herbivorous grasshoppers and caterpillars tended to exhibit lower ratios (5.0–7.8%).

Pine needles, grasses, and soils exhibited low THg, with mean concentrations of 14 ± 2.0 ng g^{-1}, 8.6 ± 2.3 ng g^{-1}, and 94 ± 52 ng g^{-1}, respectively. The mean THg concentration of pine needle was comparable to the reported value of 11 ± 7.7 ng g^{-1} from a remote pine forest (Luo et al., 2020). Unexpectedly, the THg concentration of soil in the present study was significantly higher than soil collected from a subtropical pine forest ecosystem (43 ± 11 ng g^{-1}) (Luo et al., 2020), but comparable to soils from a suburban forests (84 ± 52 ng g^{-1}) (Niu et al.,

Table 1
The concentrations of total mercury (THg), methylmercury (MeHg), ratios of methylmercury (MeHg%), stable isotope ratios ($\delta^{13}C$ and $\delta^{15}N$) and trophic levels (TL) for all samples from Changpoling Forest Park (CFP), Guizhou Province, southwest China.

Sample	THg Conc. (ng g^{-1})			MeHg Conc. (ng g^{-1})			MeHg%	$\delta^{13}C$‰	$\delta^{15}N$‰	TL
	Mean ± SD	Range	N	Mean ± SD	Range	N	Mean ± SD	Mean ± SD	Mean ± SD	
Russet Sparrow	797 ± 221	439–1267	21	388 ± 156	176–692	21	49 ± 14	−24.4 ± 0.25	4.54 ± 0.06	3.03
Green-backed Tit	521 ± 156	255–889	70	115 ± 31	67–201	70	24 ± 11	−26.2 ± 0.31	4.45 ± 0.02	3.01
Spiders[a]	433 ± 45	370–527	14	263 ± 42	208–351	14	61 ± 11	−25.5 ± 0.17	5.06 ± 0.69	3.18
Katydids[a]	37 ± 3.9	31–43	6	25 ± 4.9	19–32	6	69 ± 11	−24.8 ± 0.31	1.57 ± 0.31	2.23
Mantis[a]	30 ± 5.6	22–36	4	17 ± 5.0	13–24	4	56 ± 8.9	−19.7 ± 1.50	3.28 ± 0.38	2.69
Caterpillars[a]	32 ± 0.48	32–33	3	1.6 ± 0.18	1.4–1.8	3	5.0 ± 0.61	−31.5 ± 0.22	−0.21 ± 0.03	1.75
Grasshoppers[a]	8.2 ± 2.0	6.1–14	24	0.62 ± 0.25	0.28–1.1	19	7.8 ± 3.9	−15.2 ± 1.21	1.33 ± 0.53	2.17
Grasses	8.6 ± 2.3	5.6–12	18	0.10 ± 0.028	0.055–0.14	12	1.2 ± 0.24	−12.9 ± 0.37	−5.57 ± 1.08	1.00
Pine needles	14 ± 2.0	11–18	11	0.055 ± 0.0085	0.046–0.072	11	0.40 ± 0.077	−30.2 ± 0.70	−0.40 ± 0.07	1.00
Soil	94 ± 52	27–208	30	0.13 ± 0.11	0.017–0.55	30	0.23 ± 0.26	–	–	–

[a] Samples of invertebrates was mixed with at least 10 or more individuals.

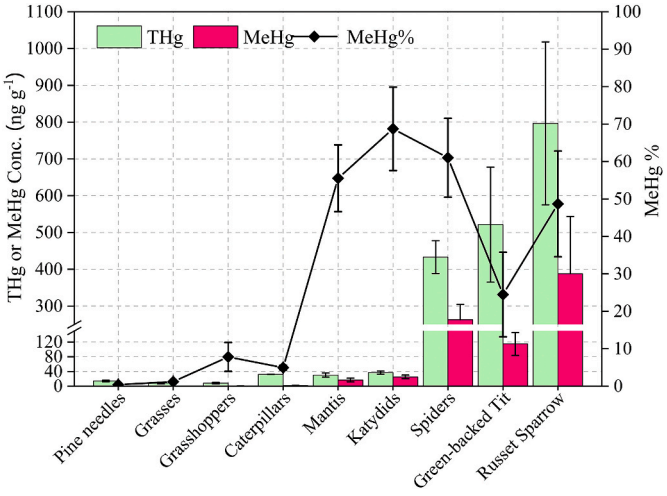

Fig. 2. Total mercury (THg, ng/g), methylmercury (MeHg, ng/g) concentrations, and the ratios of MeHg to THg (MeHg%) among all taxa.

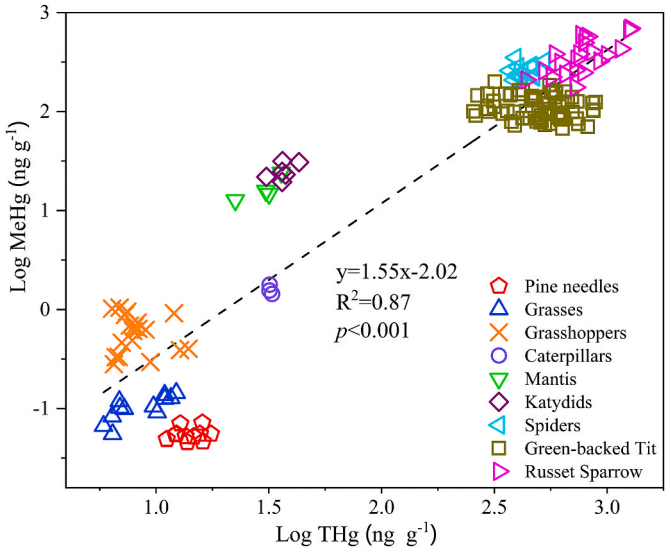

Fig. 3. Relationship between total mercury (THg) and methylmercury (MeHg) concentrations (logarithmic transformed) for all taxa.

2011). These differences in soils between urban/suburban and remote sites maybe due to the impacts from anthropogenic sources and high background in karst areas (Han et al., 2022).

Similarly, the MeHg concentrations were low in pine needles, grasses, and soils, with the concentrations in pine needles and grasses ranging from 0.046 to 0.14 ng g^{-1}, and the concentrations in soil ranging from 0.017 to 0.55 ng g^{-1}. Grasses (0.10 ± 0.028 ng g^{-1}) and pine needles (0.055 ± 0.0085 ng g^{-1}) showed the lowest average MeHg values (Table 1, Fig. 2). Similarly, low ratios of MeHg to THg were observed in both soils and plants, ranging from 0.23 ± 0.26% and 1.2 ± 0.24% on average. Relatively low THg concentrations in soils and plants might indicate a low basal input of Hg in the urban forest ecosystem of CFP.

The relationship between THg and MeHg concentrations among all taxa is shown in Fig. 3. As expected, MeHg concentrations increased with THg, and exhibited a significantly positive correlation ($R^2 = 0.87$, $p < 0.001$). The relationship observed between MeHg and THg may suggest that MeHg is driving overall THg bioaccumulation for consumers in this urban forest ecosystem (Rodenhouse et al., 2019; Tsui et al., 2019).

The Hg concentration and MeHg% in invertebrates exhibited the same order of magnitude and trend of spiders > omnivorous insects > herbivorous insects, which is comparable to previous studies on terrestrial forest food webs (Rimmer et al., 2010; Li et al., 2021; Luo et al., 2020; Tsui et al., 2019). In the present study, the THg concentrations observed in RS were similar to those reported in Leishan. However, the concentrations in GbT were 1.7 and 3.0 times higher than those observed in Leishan and Mt. Wuliang, respectively (Luo et al., 2020; Su et al., 2021). Elevated Hg levels in GbT may suggest a potential Hg source in the urban forest food web (see Section 3.3).

3.2. Characterization of urban forest food web structures

Values of $\delta^{13}C$ and $\delta^{15}N$ for all species are shown in Table 1 and Fig. 4. The caterpillars (−31.5 ± 0.22‰) and pine needles (−30.2 ± 0.70‰) had the lowest $\delta^{13}C$ values, while the highest values were observed in grasses (−12.9 ± 0.37‰) and grasshoppers (−15.2 ± 1.2‰). This suggests that the dietary carbon sources of caterpillars and grasshoppers were distinct, related to feeding on C_3 (pine needles) and C_4 (grasses) plants, respectively. Mantis (−19.7 ± 1.5‰), GbT (−26.2 ± 0.31‰), spiders (−25.5 ± 0.17‰), katydids (−24.8 ± 0.31‰), and RS (−24.4 ± 0.25‰) showed intermediate $\delta^{13}C$ values, exhibiting composite signals of C_3 and C_4 plants (Fig. 4). These results are similar to those reported for predators such as songbirds, which exhibit a variety of $\delta^{13}C$ values (Ai et al., 2019; Luo et al., 2020).

All taxa samples also showed a large range of $\delta^{15}N$ values (Fig. 4), indicating their distinct trophic positions. The three highest mean $\delta^{15}N$ values were observed in spiders (5.06 ± 0.69‰), RS (4.54 ± 0.06‰), and GbT (4.45 ± 0.02‰), followed by mantis (3.28 ± 0.38‰), katydids (1.57 ± 0.31‰), and grasshoppers (1.33 ± 0.53‰). Meanwhile, caterpillars (−0.21 ± 0.03‰), pine needles (−0.40 ± 0.07‰), and grasses (−5.57 ± 1.1‰) exhibited low values (Fig. 4). As expected, data for $\delta^{15}N$

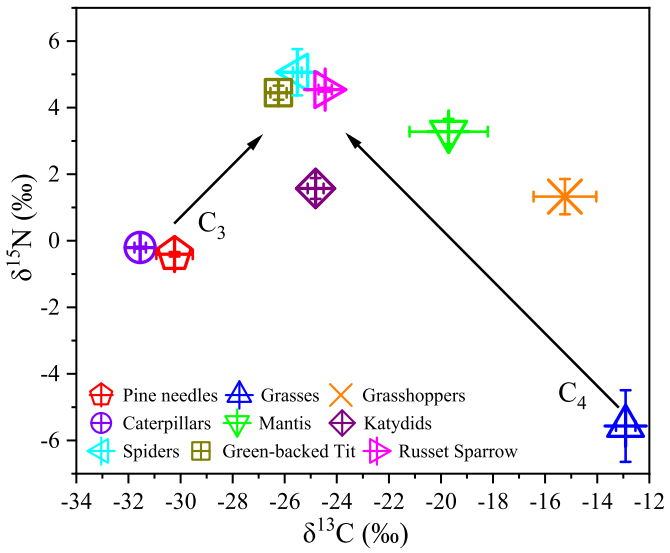

Fig. 4. Relationships between stable carbon isotope ($\delta^{13}C$) and nitrogen isotope ($\delta^{15}N$) compositions among all taxa.

in animal taxa showed the top predators of GbT, TS, and spiders at the highest trophic level, followed by mantis, katydids, and grasshoppers. The herbivorous caterpillar was the lowest. It is worth noting that the $\delta^{15}N$ fractionation values of 4.66‰ between GbT and caterpillars, and 3.12‰ between GbT and grasshoppers are not consistent with previous fractionation values of 3.7‰ (diet-seabird primary feather, Becker et al., 2007) and 3.4‰ (caterpillars-nestling feathers, Luo et al., 2020). This may be due to that the diet composition of nestling birds is different.

Based on the site-specific mean $\delta^{15}N$ value of basal resources (−2.99 ± 0.54‰) in the present study, and a mean trophic enrichment of 3.7‰ (Becker et al., 2007), which is more comparable to the average value achieved from fractionations between GbT and its diets, the TLs of consumers were estimated. Among the animal taxa, the TLs showed a range of 1.75–3.18. These levels were divided into primary consumers (second trophic level: mantis/katydids/grasshoppers/caterpillars), and top predators (third, and/or fourth trophic levels: spiders/RS/GbT), which were characterized by approximate mean TL values of 2 and 3, respectively. Hence, an urban forest food web of grasses/pine needles (plants)-grasshoppers/caterpillars/katydids/mantis (herbivorous/omnivorous)-spiders/songbirds (insectivorous) was clearly observed in the present study.

3.3. Transfer and bioaccumulation of THg and MeHg in food web

Both THg and MeHg concentrations increased with the TL, from plants to nestling birds, exhibiting distinct biomagnification through the urban forest food web. Top predators with high TLs showed greater THg and MeHg concentrations than those observed at the source.

The $BMF_{(THg)}$ and $BMF_{(MeHg)}$ of the different predators varied greatly. The $BMF_{(THg)}$ and $BMF_{(MeHg)}$ values between herbivorous/omnivorous insects and plants were 0.75–3.4 and 7.9–320, between insectivorous animals (spiders and songbirds) and herbivorous/omnivorous insects were 12–97 and 4.6–626, and between insectivorous animals (spiders and songbirds) and plants were 39–72 and 1474–4974, respectively (Fig. 5). However, within systems, the $BMF_{(MeHg)}$ value in predators was 0.33- to 69-fold, on average, higher than that of $BMF_{(THg)}$, verifying a higher preferential bioaccumulation capacity of MeHg than inorganic Hg. Less obvious differences between $BMF_{(THg)}$ and $BMF_{(MeHg)}$ in top predators (songbirds-spiders) in the present study might be due to the lower contribution of spiders to the diets of nestlings. Previous studies have demonstrated that riparian spiders can transfer aquatic Hg to arachnivorous birds via their feeding on emergent aquatic insects (Beaubien et al., 2020; Ortega-Rodriguez et al., 2019). Therefore, the uncertainty of predator-prey relationships and diet proportions may make the accurate estimation of the bioaccumulation and biomagnification of Hg in terrestrial forest food webs difficult.

In the present study, the BMFs of nestlings-plants for THg and MeHg were considerably higher than the results of nestlings-pine needles ($BMF_{(THg)}$ = 16, $BMF_{(MeHg)}$ = 114) in a remote subtropical forest (Luo et al., 2020), but consistent with the results of adult songbirds-plants ($BMF_{(THg)}$ = 40, $BMF_{(MeHg)}$ = 1795) in a remote montane area (Li et al., 2021). This suggests that efficient MeHg biomagnification exists in

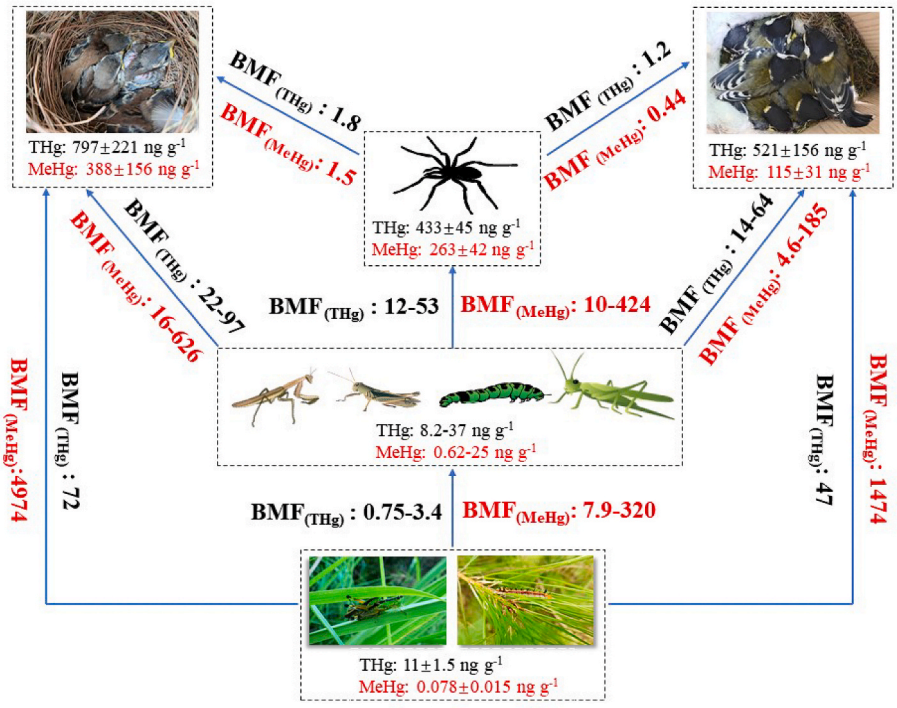

Fig. 5. The transfer patterns of total mercury (THg) and methylmercury (MeHg) in urban forest food webs. The organisms in dashed boxes were divided into different groups according to their trophic levels. The black color texts represent THg concentrations and biomagnification factors of THg ($BMF_{(THg)}$, bold). The red color texts represent MeHg concentrations and biomagnification factors of MeHg ($BMF_{(MeHg)}$, bold). The blue arrows indicate the $BMF_{(THg)}$ and $BMF_{(MeHg)}$. (For interpretation of the references to color in this figure legend, the reader is referred to the Web version of this article.)

urban forest food webs. In particular, the $BMF_{(MeHg)}$ between RS and plants was close to 5000, which is equivalent to studies observed in aquatic ecosystems (Driscoll et al., 2007).

The TMS_{THg} and TMS_{MeHg} in the urban forest food web were 0.18 ± 0.05 and 0.37 ± 0.08, respectively, suggesting that both THg and MeHg significantly increase along the food web (Fig. 6). These results are consistent with previous studies conducted in a remote subtropical pine forest in Mt. Wuliang with a pine needles-caterpillars-great tits food chain (TMS_{THg} = 0.18, TMS_{MeHg} = 0.36) (Luo et al., 2020), a subtropical montane forest food webs (TMS_{THg} = 0.22, TMS_{MeHg} = 0.38) in Mt Ailao (Li et al., 2021), and a rice-herbivorous insects-carnivorous insects-birds food web (TMS_{THg} = 0.40, TMS_{MeHg} = 0.36) in heavily Hg-contaminated sites (Abeysinghe et al., 2017). However, these values are significantly higher than values obtained in a temperate terrestrial-aquatic forest food web (TMS_{THg} = 0.14, TMS_{MeHg} = 0.09) in New Hampshire, USA (Rodenhouse et al., 2019) and freshwater food webs (TMS_{THg} = 0.16, TMS_{MeHg} = 0.24) in a global meta-analysis (Lavoie et al., 2013).

Interestingly, GbT exhibited approximately 3.0 and 8.2 times higher THg and MeHg concentrations, respectively, than those from Mt. Wuliang, reported by Luo et al. (2020). Although the eco-regions of CFP and Mt. Wuliang have similar Hg levels in plants and invertebrates, and similar TMS values for THg and MeHg, the elevated Hg concentrations in GbTs are likely attributed to the differences in food sources and food web structures. Thus, the intense anthropogenic activities in urban forests may potentially alters the bioaccumulation of Hg in songbirds. In addition, some researchers have considered the possibility of maternal transfer of Hg to nestlings via laying eggs (Ackerman et al., 2017, 2020). Hence, an alternative explanation is maternal transfer across the egg to the nestling. Further studies are required to confirm the contributions of maternal-derived Hg or dietary Hg to the elevated Hg in GbT. This result may also imply that the songbird species of GbT is more sensitive to environmental Hg exposure than other species.

Actually, some uncertainties existed as the recoveries of MeHg were slightly higher than 100%. We also discussed the uncertainties caused by the slightly positive bias in MeHg analysis, and evaluated the potential impacts on our key conclusions that including the correlation analysis between LogTHg and LogMeHg concentrations and results of TMS_{MeHg} (the slope of the regressions of LogMeHg on $\delta^{15}N$). The results suggested that the slightly positive recoveries of MeHg have limited impacts on these key conclusions, which even can be ignored (the details are shown in Supporting Information).

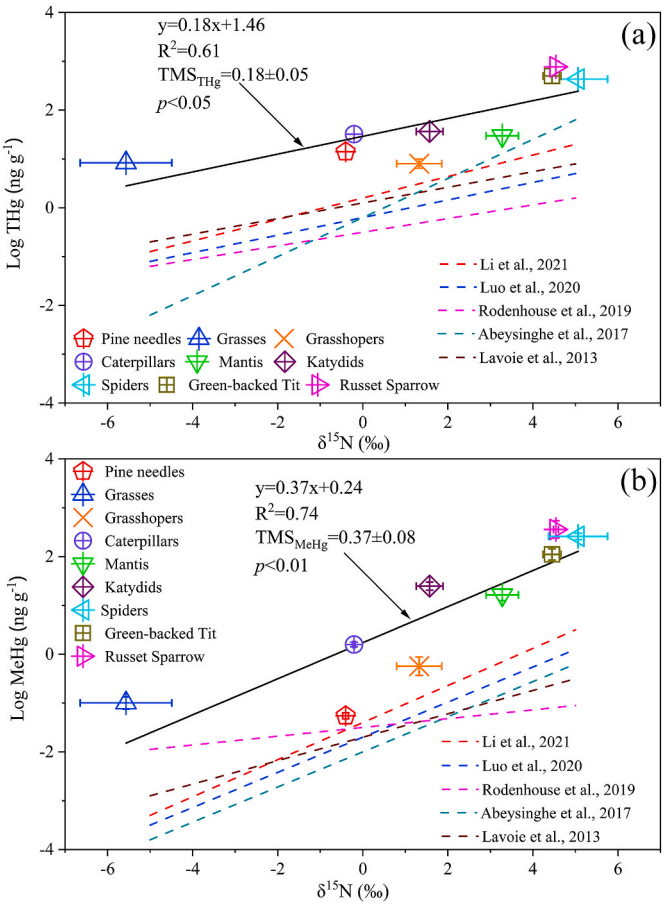

Fig. 6. The correlations between stable nitrogen isotopes ($\delta^{15}N$) and logTHg (a), logMeHg (b) concentrations across all taxa. The trophic magnification slope (TMS) was the slope of the regressions of log [THg] or log [MeHg] on $\delta^{15}N$. The slopes of the dashed line represent the TMS values from other studies.

4. Conclusions

This study of an urban forest terrestrial ecosystem revealed significant bioaccumulation and transfer magnification of THg and MeHg in the grasses/pine needles-grasshoppers/caterpillars/katydids/mantis-spiders/songbirds food web. The Hg concentrations in nestling songbirds were higher than those in background regions characterized by similar primary basal resources of Hg. High BMF values (up to 5000 for MeHg) and TMS indicated stronger biomagnification in the urban forest food web than those in background regions. The results from primary consumers suggest that the bioaccumulation of Hg in songbirds also suffered from a higher risk of Hg exposure due to the inhabit urban forests expose to intensively anthropogenic activities. Our findings provide a primary understanding of biogeochemical Hg cycles in terrestrial food webs, emphasizing the importance of studying the Hg cycle in urban forests. Future studies on stable Hg isotope compositions in organisms varying in trophic positions in the food web would contribute to a better understanding of the cycling of MeHg in urban forest ecosystems.

Credit author statement

Fudong Zhang: Methodology, Formal analysis, Investigation, Data curation, Writing - original draft, Visualization. **Zhidong Xu:** Investigation, Methodology, Writing - review& editing, Visualization, Funding acquisition. **Xiaohang Xu:** Validation, Formal analysis, Writing - review& editing, Funding acquisition. **Zhuo Chen:** Conceptualization, Supervision, Writing - review& editing. **Longchao Liang:** Investigation, Data curation. **Xian Dong:** Investigation, Data curation. **Kang Luo:** Methodology, Investigation, Resources. **Faustino Dinis:** Methodology, Investigation. **Guangle Qiu:** Conceptualization, Writing - review& editing, Supervision, Project administration, Funding acquisition.

Declaration of competing interest

The authors declare that they have no know competing financial interests or personal relationships that could have appeared to influence the work reported in this paper.

Acknowledgements

This work was supported by the Program of Department of Science and Technology of Guizhou Province (QianKeHe[2019]2307), Guizhou Provincial 2020 Science and Technology Subsidies (No. GZ2020SIG), and the National Natural Science Foundation of China (NSFC: 41573135, 42003065, and 42103080). We greatly thank the support and assistance for the nest boxes installation and sample site management from Administrations of Duxi Forest Farm, Administrations of Changpoling National Forest Park and Natural Resource Bureau of Baiyun District of Guiyang City, Guizhou Province. We also thank Jialiang Han, Lin Liu, Gaoen Wu, Chan Li, Lin Kong, Hongmei Wu, Yuxiao Shao, Taiwen Zhang and Shenghao Li for their help in sample collection

and laboratory work. We greatly appreciate the constructive comments from three anonymous reviewers. We greatly appreciate Dr. Wei Yuan for his help in the article revising.

Appendix A. Supplementary data

Supplementary data to this article can be found online at https://doi.org/10.1016/j.chemosphere.2022.134424.

References

Abeysinghe, K.S., Qiu, G., Goodale, E., Anderson, C.W.N., Bishop, K., Evers, D.C., Goodale, M.W., Hintelmann, H., Liu, S., Mammides, C., Quan, R.C., Wang, J., Wu, P., Xu, X.H., Yang, X.D., Feng, X., 2017. Mercury flow through an Asian rice-based food web. Environ. Pollut. 229, 219–228.

Ackerman, J.T., Hartman, C.A., Herzog, M.P., 2017. Maternal transfer of mercury to songbird eggs. Environ. Pollut. 230, 463–468.

Ackerman, J.T., Herzog, M.P., Evers, D.C., Cristol, D.A., Kenow, K.P., Heinz, G.H., Lavoie, R.A., Brasso, R.L., Mallory, M.L., Provencher, J.F., Braune, B.M., Matz, A., Schmutz, J.A., Eagles-Smith, C.A., Savoy, L.J., Meyer, M.W., Hartman, C.A., 2020. Synthesis of maternal transfer of mercury in birds: implications for altered toxicity risk. Environ. Sci. Technol. 54, 2878–2891.

Adams, E.M., Sauer, A.K., Lane, O., Regan, K., Evers, D.C., 2020. The effects of climate, habitat, and trophic position on methylmercury bioavailability for breeding New York songbirds. Ecotoxicology 29, 1843–1861.

Ai, S., Yang, Y., Ding, J., Yang, W., Bai, X., Bao, X., Ji, W., Zhang, Y., 2019. Metal exposure risk assessment for tree sparrows at different life stages via diet from a polluted area in northwestern China. Environ. Toxicol. Chem. 38, 2785–2796.

Azemard, S., Vassileva, E., 2021. Rapid determination of femtomolar methylmercury in seawater using automated GC-AFS method: optimisation of the extraction step and method validation. Talanta 232, 122492.

Beaubien, G.B., Olson, C.I., Todd, A.C., Otter, R.R., 2020. The spider exposure pathway and the potential risk to arachnivorous birds. Environ. Toxicol. Chem. 39, 2314–2324.

Becker, B.H., Newman, S.H., Inglis, S., Beissinger, S.R., 2007. Diet–feather stable isotope ($\delta^{15}N$ and $\delta^{13}C$) fractionation in common murres and other seabirds. Condor 109, 451–456.

Cristol, D.A., Brasso, R.L., Condon, A.M., Fovargue, R.E., Friedman, S.L., Hallinger, K.K., Monroe, A.P., White, A.E., 2008. The movement of aquatic mercury through terrestrial food webs. Science 320, 335.

Driscoll, C.T., Han, Y.J., Chen, C.Y., Evers, D.C., Lambert, K.F., Holsen, T.M., Kamman, N.C., Munson, R.K., 2007. Mercury contamination in forest and freshwater ecosystems in the Northeastern United States. Bioscience 57, 17–28.

Driscoll, C.T., Mason, R.P., Chan, H.M., Jacob, D.J., Pirrone, N., 2013. Mercury as a global pollutant: sources, pathways, and effects. Environ. Sci. Technol. 47, 4967–4983.

Eagles-Smith, C.A., Silbergeld, E.K., Basu, N., Bustamante, P., Diaz-Barriga, F., Hopkins, W.A., Kidd, K.A., Nyland, J.F., 2018. Modulators of mercury risk to wildlife and humans in the context of rapid global change. Ambio 47, 170–197.

FAO, 2016. Guidelines on urban and peri-urban forestry. In: Salbitano, F., Borelli, S., Conigliaro, M., Chen, Y. (Eds.), FAO Forestry Paper No. 178. Rome, Food and Agriculture Organiztion of the United Nations.

Fitzgerald, W.F., Engstrom, D.R., Mason, R.P., Nater, E.A., 1998. The case for atmospheric mercury contamination in remote areas. Environ. Sci. Technol. 32, 1–7.

Fry, B., 2006. Stable Isotope Ecology. Springer, New York.

Gentes, S., Lohrer, B., Legeay, A., Mazel, A.F., Anschutz, P., Charbonnier, C., Tessier, E., Maury-Brachet, R., 2021. Drivers of variability in mercury and methylmercury bioaccumulation and biomagnification in temperate freshwater lakes. Chemosphere 267, 128890.

Hammerschmidt, C.R., Fitzgerald, W.F., 2005. Methylmercury in mosquitoes related to atmospheric mercury deposition and contamination. Environ. Sci. Technol. 39, 3034–3039.

Han, J., Liang, L., Zhu, Y., Xu, X., Wang, L., Shang, L., Wu, P., Wu, Q., Qian, X., Qiu, G., Feng, X., 2022. Heavy metal(loid)s in farmland soils in the karst plateau, Southwest China: an integrated analysis of geochemical baselines, source apportionment and associated health risk. Land Degrad. Dev. https://doi.org/10.1002/ldr.4257. In press.

Hintelmann, H., Nguyen, H.T., 2005. Extraction of methylmercury from tissue and plant samples by acid leaching. Anal. Bioanal. Chem. 381, 360–365.

Horvat, M., Degenek, N., Lipej, L., Snoj Tratnik, J., Faganeli, J., 2014. Trophic transfer and accumulation of mercury in ray species in coastal waters affected by historic mercury mining (Gulf of Trieste, northern Adriatic Sea). Environ. Sci. Pollut. Control Ser. 21, 4163–4176.

Horvat, M., Nolde, N., Fajon, V., Jereb, V., Logar, M., Lojen, S., Jacimovic, R., Falnoga, I., Liya, Q., Faganeli, J., Drobne, D., 2003. Total mercury, methylmercury and selenium in mercury polluted areas in the province Guizhou, China. Sci. Total Environ. 304, 231–256.

Hsu-Kim, H., Eckley, C.S., Achá, D., Feng, X., Gilmour, C.C., Jonsson, S., Mitchell, C.P.J., 2018. Challenges and opportunities for managing aquatic mercury pollution in altered landscapes. Ambio 47, 141–169.

Jackson, A.K., Evers, D.C., Adams, E.M., Cristol, D.A., Eagles-Smith, C., Edmonds, S.T., Gray, C.E., Hoskins, B., Lane, O.P., Sauer, A., Tear, T., 2015. Songbirds as sentinels of mercury in terrestrial habitats of eastern North America. Ecotoxicology 24, 453–467.

Kidd, K.A., Muir, D.C., Evans, M.S., Wang, X., Whittle, M., Swanson, H.K., Johnston, T., Guildford, S., 2012. Biomagnification of mercury through lake trout (Salvelinus namaycush) food webs of lakes with different physical, chemical and biological characteristics. Sci. Total Environ. 438, 135–143.

Lavoie, R.A., Jardine, T.D., Chumchal, M.M., Kidd, K.A., Campbell, L.M., 2013. Biomagnification of mercury in aquatic food webs: a worldwide meta-analysis. Environ. Sci. Technol. 47, 13385–13394.

Li, C., Xu, Z., Luo, K., Chen, Z., Xu, X., Xu, C., Qiu, G., 2021. Biomagnification and trophic transfer of total mercury and methylmercury in a sub-tropical montane forest food web, southwest China. Chemosphere 277, 130371.

Liang, L., Horvat, M., Bloom, N.S., 1994. An improved speciation method for mercury by GC/CVAFS after aqueous phase ethylation and room temperature precollection. Talanta 41, 371–379.

Liang, L., Horvat, M., Feng, X.B., Shang, L.H., Lil, H., Pang, P., 2004. Re-evaluation of distillation and comparison with HNO_3 leaching/solvent extraction for isolation of methylmercury compounds from sediment/soil samples. Appl. Organomet. Chem. 18, 264–270.

Livesley, S.J., McPherson, G.M., Calfapietra, C., 2016. The urban forest and ecosystem services: impacts on urban water, heat, and pollution cycles at the tree, street, and city scale. J. Environ. Qual. 45, 119–124.

Low, K.E., Ramsden, D.K., Jackson, A.K., Emery, C., Robinson, W.D., Randolph, J., Eagles-Smith, C.A., 2020. Songbird feathers as indicators of mercury exposure: high variability and low predictive power suggest limitations. Ecotoxicology 29, 1281–1292.

Luo, K., Xu, Z., Wang, X., Quan, R., Lu, Z., Bi, W., Zhao, H., Qiu, G., 2020. Terrestrial methylmercury bioaccumulation in a pine forest food chain revealed by live nest videography observations and nitrogen isotopes. Environ. Pollut. 263, 114530.

Ma, Y., Zheng, W., An, Y., Chen, L., Xu, Q., Jiang, A., 2021. Mercury contamination in terrestrial predatory birds from Northeast China: implications for species and feather type selection for biomonitoring. Ecol. Indicat. 130, 108108.

Niu, Z., Zhang, X., Wang, Z., Ci, Z., 2011. Mercury in leaf litter in typical suburban and urban broadleaf forests in China. J. Environ. Sci. (China) 23, 2042–2048.

Obrist, D., Roy, E.M., Harrison, J.L., Kwong, C.F., Munger, J.W., Moosmuller, H., Romero, C.D., Sun, S., Zhou, J., Commane, R., 2021. Previously unaccounted atmospheric mercury deposition in a midlatitude deciduous forest. Proc. Natl. Acad. Sci. U. S. A. 118 e2105477118.

Ortega-Rodriguez, C.L., Chumchal, M.M., Drenner, R.W., Kennedy, J.H., Nowlin, W.H., Barst, B.D., Polk, D.K., Hall, M.N., Williams, E.B., Lauck, K.C., Santa-Rios, A., Basu, N., 2019. Relationship between methylmercury contamination and proportion of aquatic and terrestrial prey in diets of shoreline spiders. Environ. Toxicol. Chem. 38, 2503–2508.

Peterson, S.H., Ackerman, J.T., Toney, M., Herzog, M.P., 2019. Mercury concentrations vary within and among individual bird feathers: a critical evaluation and guidelines for feather use in mercury monitoring programs. Environ. Toxicol. Chem. 38, 1164–1187.

Post, D.M., 2002. Using stable isotopes to estimate trophic position: models, methods, and assumptions. Ecology 83, 703–718.

Richardson, J.B., Moore, L., 2020. A tale of three cities: mercury in urban deciduous foliage and soils across land-uses in Poughkeepsie NY, Hartford CT, and Springfield MA USA. Sci. Total Environ. 715, 136869.

Rimmer, C.C., Miller, E.K., McFarland, K.P., Taylor, R.J., Faccio, S.D., 2010. Mercury bioaccumulation and trophic transfer in the terrestrial food web of a montane forest. Ecotoxicology 19, 697–709.

Rodenhouse, N.L., Lowe, W.H., Gebauer, R.L.E., McFarland, K.P., Bank, M.S., 2019. Mercury bioaccumulation in temperate forest food webs associated with headwater streams. Sci. Total Environ. 665, 1125–1134.

Scheuhammer, A.M., Meyer, M.W., Sandheinrich, M.B., Murray, M.W., 2007. Effects of environmental methylmercury on the health of wild birds, mammals, and fish. Ambio 36, 12–18.

Su, T., He, C., Jiang, A., Xu, Z., Goodale, E., Qiu, G., 2021. Passerine bird reproduction does not decline in a highly-contaminated mercury mining district of China. Environ. Pollut. 286, 117440.

Tsui, M.T.K., Blum, J.D., Kwon, S.Y., Finlay, J.C., Balogh, S.J., Nollet, Y.H., 2012. Sources and transfers of methylmercury in adjacent river and forest food webs. Environ. Sci. Technol. 46, 10957–10964.

Tsui, M.T.K., Adams, E.M., Jackson, A.K., Evers, D.C., Blum, J.D., Balogh, S.J., 2018. Understanding sources of methylmercury in songbirds with stable mercury isotopes: challenges and future directions. Environ. Toxicol. Chem. 37, 166–174.

Tsui, M.T.K., Liu, S., Brasso, R.L., Blum, J.D., Kwon, S.Y., Ulus, Y., Nollet, Y.H., Balogh, S. J., Eggert, S.L., Finlay, J.C., 2019. Controls of methylmercury bioaccumulation in forest floor food webs. Environ. Sci. Technol. 53, 2434–2440.

US EPA, 1998. Method 1630: Methyl Mercury in Water by Distillation, Aqueous Ethylation, Purge and Trap, and Cold Vapor Atomic Fluorescence Spectrometry. U.S. EPA, Washington, D.C, USA, pp. 1–55.

US EPA, 2002. Method 1631E: Mercury in Water by Oxidation, Purge and Trap, and Cold Vapor Atomic Fluorescence Spectrometry. U.S. EPA, Washington, D.C, USA, pp. 1–46.

US EPA, 2007. Method 7473: Mercury in Solids and Solutions by Thermal Decomposition, Amalgamation, and Atomic Absorption Spectrophotometry. U.S. EPA, Washington, D.C, USA, pp. 1–17.

Wang, X., Bao, Z., Lin, C.J., Yuan, W., Feng, X., 2016. Assessment of global mercury deposition through litterfall. Environ. Sci. Technol. 50, 8548–8557.

Wang, X., Yuan, W., Lin, C.J., Luo, J., Wang, F., Feng, X., Fu, X., Liu, C., 2020. Underestimated sink of atmospheric mercury in a deglaciated forest chronosequence. Environ. Sci. Technol. 54, 8083–8093.

Watras, C.J., Back, R.C., Halvorsen, S., Hudson, R.J.M., Morrison, K.A., Wente, S.P., 1998. Bioaccumulation of mercury in pelagic freshwater food webs. Sci. Total Environ. 219, 183–208.
Willacker, J.J., Eagles-Smith, C.A., Kowalski, B.M., Danehy, R.J., Jackson, A.K., Adams, E.M., Evers, D.C., Eckley, C.S., Tate, M.T., Krabbenhoft, D.P., 2019. Timber harvest alters mercury bioaccumulation and food web structure in headwater streams. Environ. Pollut. 253, 636–645.
Yung, L., Bertheau, C., Cazaux, D., Regier, N., Slaveykova, V.I., Chalot, M., 2019. Insect life traits are key factors in mercury accumulation and transfer within the terrestrial food web. Environ. Sci. Technol. 53, 11122–11132.
Zabala, J., Meade, A.M., Frederick, P., 2019. Variation in nestling feather mercury concentrations at individual, brood, and breeding colony levels: implications for sampling mercury in birds. Sci. Total Environ. 671, 617–621.
Zhang, Z., Wang, Q., Zheng, D., Zheng, N., Lu, X., 2010. Mercury distribution and bioaccumulation up the soil-plant-grasshopper-spider food chain in Huludao City, China. J. Environ. Sci. (China) 22, 1179–1183.
Zhou, J., Wang, Z., Sun, T., Zhang, H., Zhang, X., 2016. Mercury in terrestrial forested systems with highly elevated mercury deposition in southwestern China: the risk to insects and potential release from wildfires. Environ. Pollut. 212, 188–196.